

## 산소/질소 분리를 위한 다층구조 제올라이트 5A를 함유한 탄소분자체 분리막 제조

리 웬<sup>\*.1</sup> · 추 아 충 양<sup>\*\*1</sup> · 배 태 현<sup>\*,\*\*,\*.\*.\*.\*.†</sup>

\*싱가포르 난양이공대학교 화학생명공학부, \*\*싱가포르 분리막 센터, \*\*\*한국과학기술원 생명화학공학과  
(2020년 7월 16일 접수, 2020년 8월 5일 수정, 2020년 8월 8일 채택)

### Hierarchical 5A Zeolite-Containing Carbon Molecular Sieve Membranes for O<sub>2</sub>/N<sub>2</sub> Separation

Wen Li<sup>\*.1</sup>, Chong Yang Chuah<sup>\*\*1</sup>, and Tae-Hyun Bae<sup>\*,\*\*,\*.\*.\*.\*.†</sup>

\*School of Chemical and Biomedical Engineering, Nanyang Technological University, Singapore 637459, Singapore  
\*\*Singapore Membrane Technology Centre, Nanyang Technological University, Singapore 637141, Singapore  
\*\*\*Department of Chemical and Biomolecular Engineering, Korea Advanced Institute of Science and Technology,  
Daejeon 34141, Republic of Korea

(Received July 16, 2020, Revised August 5, 2020, Accepted August 8, 2020)

**요약:** 다층 구조를 가진 5A 제올라이트를 탄소 분자체 분리막에 첨가한 복합막을 제조하고 질소/산소의 분리 특성을 평가하였다. 제올라이트의 첨가는 선택도에는 미세한 영향을 주지만 투과도를 크게 증가시키는 방법으로 전체적인 탄소막의 질소/산소의 분리 성능을 상승시켰다. 특히 메조포어를 함유한 다층구조의 제올라이트 첨가체는 분리막의 투과도를 보다 효율적으로 상승시켜 아주 우수한 분리 성능에 도달하였다. 이 연구의 결과는 저렴한 탄소막 전구체와 제올라이트 소재를 활용하고도 고성능의 질소/산소 분리막을 손쉽게 제조할 수 있다는 것을 제시한다.

**Abstract:** Mixed-matrix carbon molecular sieve membranes containing conventional and hierarchically structured 5A were synthesized for application in oxygen (O<sub>2</sub>)/nitrogen (N<sub>2</sub>) separation. In general, incorporating 5A fillers into porous carbon matrices dramatically increased the permeability of the membrane with a marginal decrease in selectivity, resulting in very attractive O<sub>2</sub>/N<sub>2</sub> separation performances. Hierarchical zeolite 5A, which contains both microporous and mesoporous domains, improved the separation performance further, indicating that the mesopores in the zeolite can serve as an additional path for rapid gas diffusion without sacrificing O<sub>2</sub>/N<sub>2</sub> selectivity substantially. This facile strategy successfully and cost-effectively pushed the performance close to the Robeson upper bound. It produced high performance membranes based on Matrimid<sup>®</sup> 5218 polyimide and zeolite 5A, which are inexpensive commercial products.

**Keywords:** hierarchical zeolite, carbon molecular sieve membrane, O<sub>2</sub>/N<sub>2</sub> separation, mixed-matrix membrane

#### 1. Introduction

In recent years, air separation processes have played a pivotal role in numerous industrial applications such as the production of primary metals (non-ferrous metals or steel), fuel combustion, gasification, petrochemical production, and glass and concrete production. For

instance, high-purity oxygen (O<sub>2</sub>) is preferred for oxy-fuel combustion, as it provides a higher energy efficiency than compressed air, as nitrogen (N<sub>2</sub>) typically acts as a non-reactive gas that is not actively involved in the combustion process[1]. O<sub>2</sub> is also heavily used to lower the carbon content of iron-steel alloys, which leads to the formation of low-carbon steel[2]. The highly

†Corresponding author(e-mail: thbae@kaist.ac.kr, <https://orcid.org/0000-0003-0033-2526>)

<sup>1</sup>These authors contributed equally to this work.

inert properties of N<sub>2</sub> ensure its capability to act as a shielding gas during the degassing of molten metals, thus preventing any significant presence of oxidizing components (e.g., oxygen and moisture) that can lead to the oxidation of metals at elevated temperatures[3]. N<sub>2</sub> can also be used in food packing processes to preserve food for a long time[4].

In general, several methodologies have been developed to effectively conduct the air separation process. Distillation, the conventional cryogenic air separation process, has been actively used by major industrial gas companies due to its large-scale O<sub>2</sub> production capability[5-7]. Pressure swing adsorption or vacuum pressure swing adsorption can also be used to generate O<sub>2</sub> with high purity via the use of adsorbents that allow selective adsorption[8-10]. Nevertheless, these technologies have substantial limitations in terms of high capital and operating costs as well as high energy consumption. Hence, a membrane-based separation process has been considered a promising alternative due to its cost effectiveness, simplicity, and small plant footprint.

Until now, polymeric membranes have been heavily used in the gas separation process, due to their high mechanical strength, high chemical resistance, and ease of fabrication. In addition, polymeric membranes can be fabricated into multiple membrane configurations such as flat sheets, spiral wounds, and hollow fiber modules. Nonetheless, the well-known permeability-selectivity trade-off, demonstrated in the Robeson plot [11,12], is the typical behavior of polymeric membranes, as the gas transport properties of membranes are governed by the solution-diffusion mechanism. Under this plot, an upper bound is constructed to demonstrate the limit of gas separation performance of polymeric membranes. Researchers have investigated several approaches that move the performance towards the upper bound limit. Among them, the carbonization of polymer precursors has been studied as an effective method for developing high-performance membranes[13-15]. However, the selection of an appropriate carbonization condition is generally dependent on several factors, such as type of inert flow gases (helium, nitrogen, ar-

gon), ramping rate, pyrolysis temperature, and soaking time[16,17]. In addition, it is well-known that the performance of such carbon molecular sieve membranes (CMSMs) is strongly dependent on the choice of polymer precursors. For instance, membranes that are derived from glassy polymers with high fractional free volume such as 6FDA (4,4'-(hexafluoro-isopropylidene) diphthalic anhydride) containing polyimides tend to give extraordinary gas separation performance. However, the harsh synthesis conditions and high costs generally limit the industrial applications of these polymers[17-19].

Therefore, we have adopted an approach that involves the carbonization of polymer precursors incorporating inorganic nanoporous fillers to form mixed-matrix CMSMs[20-24]. The polymer precursor selected for this study was Matrimid<sup>®</sup> 5218, as it is more readily available than the other glassy polymers (e.g., 6FDA-based polymer[19]) that require sophisticated synthesis procedures. Meanwhile, zeolite 5A, which possesses a well-defined micropore 4.8 Å[25], was chosen as the filler materials. The pore structures of 5A zeolite fillers were systematically controlled to optimize the gas separation performance. It has been suggested that the creation of hierarchical microporous-mesoporous domains is an attractive alternative method, given the possibility that small micropore channels limit the accessibility of gas molecules, leading to a slow pore diffusion[26,27]. It should be noted that zeolite LTA can be readily synthesized in the form of hierarchically porous structure by using the soft templating method. In addition, instead of as-made LTA zeolite (Na-A) that can slow down the diffusions of O<sub>2</sub> and N<sub>2</sub> due to its small pore (3.8 Å), zeolite 5A possessing a larger pore can be deliberately used with an aim to improve the permeability of a CMSM which already has a good O<sub>2</sub>/N<sub>2</sub> selectivity.

Based on the rationale mentioned above, we fabricated mixed-matrix CMSMs using Matrimid<sup>®</sup> 5218 carbon precursors and zeolite 5A fillers with a variety of physical properties (zeolite 5A and hierarchical zeolite 5A) for the application in O<sub>2</sub>/N<sub>2</sub> separation. Then, the effect of zeolite 5A fillers on O<sub>2</sub>/N<sub>2</sub> separation performance

was studied in a systematic manner, focusing on the impact of mesoporosity that was introduced into the zeolite particles. The membranes prepared with this facile method gave outstanding performances that were far better than the pure CMSM, indicating that the strategy tested in this study is highly suitable for industrial applications.

## 2. Experiment

### 2.1. Materials

Calcium nitrate tetrahydrate ( $\text{Ca}(\text{NO}_3)_2 \cdot 4\text{H}_2\text{O}$ ), dimethyloctadecyl[3-(trimethoxysilyl)propyl] ammonium chloride solution (TPOAC, 42 wt% in methanol), sodium aluminate (Al: 50~56%, Na: 37~45%), aluminium isopropoxide ( $\geq 98.0\%$ ), sodium hydroxide ( $\geq 98.5\%$ ), sodium metasilicate pentahydrate ( $\geq 95.0\%$ ), Ludox<sup>®</sup> HS-40 colloidal silica (40 wt% suspension in  $\text{H}_2\text{O}$ ), and tetramethylammonium hydroxide (TMAOH, 25 wt% in  $\text{H}_2\text{O}$ ) were purchased from Sigma-Aldrich. Chloroform ( $\geq 99.8\%$ ) was purchased from VWR. The chemicals and solvents were used as received, without further purifications. Matrimid<sup>®</sup> 5218 was purchased from Huntsman Chemicals, and the polymer powder was dried at 180 °C under vacuum prior to use. Deionized (DI) water was produced in-house. Argon gas (Ar,  $\geq 99.9995\%$ ), helium gas (He,  $\geq 99.9995\%$ ), and  $\text{O}_2/\text{N}_2$  (21/79 by volume) mixed gas were purchased from Airliquide.

### 2.2. Synthesis of zeolites

The zeolite LTA and hierarchical zeolite LTA were synthesized using the methods described in the literature[28]. For the preparation of hierarchical zeolite LTA (H-LTA), the precursor solution was prepared with a molar ratio of 10  $\text{Al}_2\text{O}_3/40 \text{Na}_2\text{O}/15 \text{SiO}_2/2400 \text{H}_2\text{O}/1.25 \text{TPOAC}$  under ambient conditions. First, two separate solutions were prepared. One solution was a mixture of sodium metasilicate pentahydrate, sodium hydroxide, TPOAC, and deionized (DI) water, and the second solution was prepared by dissolving sodium aluminate in DI water. After the two solutions were completely homogeneous, the solutions were mixed to-

gether and heated at 100°C for 4 h via vigorous agitation. Once the reaction was completed, the product was collected using vacuum filtration, and it was washed with copious amounts of DI water to remove the undesired impurities. Then, the product was dried at 100°C overnight in a convection oven. Next, the sample was calcined in a furnace at 550°C for 3 h with a ramping rate of 1 °C/min. This step was required to remove the TPOAC that was present in the samples, thus creating hierarchical zeolite LTA. Similarly, zeolite LTA was synthesized using the same procedures as for hierarchical zeolite LTA, but without the addition of TPOAC. The molar ratio of the precursor solution was controlled to be 10  $\text{Al}_2\text{O}_3/40 \text{Na}_2\text{O}/15 \text{SiO}_2/2400 \text{H}_2\text{O}$ .

Subsequently, ion exchange was conducted to convert the zeolite LTA (4A, with  $\text{Na}^+$ ) to zeolite 5A (with  $\text{Ca}^{2+}$ ). Specifically, 1 g of zeolite LTA was dispersed in 50 mL of 0.5 M  $\text{Ca}(\text{NO}_3)_2$  solution and vigorously stirred at 60°C for 12 h. This ion-exchange procedure was repeated twice to ensure a higher degree of substitution to  $\text{Ca}^{2+}$ . Finally, the zeolite 5A and hierarchical zeolite 5A was collected using vacuum filtration, and the product was dried at 80°C overnight.

### 2.3. Synthesis of carbon molecular sieve membranes derived from polymeric and mixed-matrix membranes

Polymeric and mixed-matrix flat sheet precursor membranes were fabricated using a solution-casting technique that has been reported in previous studies[29,30]. For the synthesis of polymeric membranes, a dope solution was prepared by dissolving dry Matrimid<sup>®</sup> 5218 powder in chloroform, with the concentration of the polymer solution set at around 15 wt%. The dope solution for the mixed-matrix membranes was prepared using the following steps. The zeolites were first ground before being dispersed in a chloroform solution. To reduce the aggregation and improve the overall homogeneity of the zeolites in the dope solution, sonication horn (Qsonica, Q125) was used. Subsequently, dry Matrimid<sup>®</sup> 5218 powder was added to the solution, followed by vigorous stirring until it was completely

dissolved. Next, the dope solution was cast onto a glass plate with the aid of a casting knife. The casting process was conducted in a glove bag which is filled with chloroform vapor to slow down the solvent evaporation. The flat sheet precursor membranes were annealed at 180°C in a vacuum overnight to remove any residual solvents present in the sample. Subsequently, the membrane carbonization process was conducted to form carbon molecular sieve membranes in a tube furnace (Carbolite GERO, CTF 12/100/900). Prior to the carbonization process, Ar was purged into the quartz tube (> 1 h) to remove any residual air and moisture present inside the tube. Then, the membrane precursors were carbonized using a two-step ramping procedure (380°C for 0.5 h at a rate of 2 °C/min and 550°C for 2 h at a rate of 0.5 °C/min). The carbonized membranes were cooled to room temperature after the process was completed.

#### 2.4. Characterization

The morphologies of the zeolites and the cross-section morphologies of the carbon molecular sieve membranes were observed using field emission-scanning electron microscopy (FE-SEM, JSM6701 JOEL). X-ray diffraction (PXRD) patterns of the zeolites and carbon molecular sieve membranes were measured using a Bruker D2 phaser diffractometer with a Cu-K  $\alpha$  source (1.5418 Å) in the  $2\theta$  range of 5~50°. The thermal stabilities of the zeolites and membrane precursors were determined via a thermogravimetric/differential thermal analyzer (TG/DTA), (SDT Q600, TA Instrument) within a temperature range of 40 to 900°C. The measurements were conducted under pure N<sub>2</sub> purging at 100 ml/min, with a heating rate of 10 °C/min. N<sub>2</sub> physisorption measurement (Autosorb 6B, Quantachrome) of zeolites was conducted at -196°C (77 K) under the relative pressure ( $P/P^0$ ) range of 0~1 bar to investigate the porosity properties of the zeolites. The zeolites were activated at 250°C for 24 h under a high vacuum prior to the measurement. The O<sub>2</sub> and N<sub>2</sub> adsorption isotherms of the zeolites were measured using a volumetric gas sorption analyzer (iSorb HP1, Quantachrome)

at 35°C in the pressure range of 0~1 bar after the activation conducted under the same activation conditions mentioned above.

#### 2.5. Mixture gas permeation

A gas permeation test was carried out using the constant pressure-variable volume system developed by GTR Tec Corporation. The membrane was first mounted onto the permeation cell with the temperature set to 35°C. Throughout the analysis, a binary O<sub>2</sub>/N<sub>2</sub> mixture (21/79 by volume) and helium were flown continuously in the upstream and downstream, respectively, with the flow rate controlled by the mass flow controllers. At a periodic time interval, the gas in the downstream (a mixture of the permeated gas and He) was injected into the gas chromatography to analyze its composition. This process was repeated until the concentrations of O<sub>2</sub> and N<sub>2</sub> were no longer fluctuated. The measurement was repeated for at least three samples for each pure polymeric membrane and mixed-matrix membrane to ensure the reproducibility of the gas permeation results.

### 3. Results and Discussion

#### 3.1. Properties of zeolites

The overall morphologies of the zeolite samples that are synthesized in this study are illustrated in Fig. 1(a) and (b). In general, zeolite 5A has a uniform structural topology; the typical cubic LTA crystals illustrated in Fig. 1(a) when TPOAC was not added to the precursor gel during the synthesis. In contrast, the overall shape of the particle was converted to a spherical shape (from a cubical shape) when TPOAC was incorporated into the reagent mixture. Based on the FE-SEM images, the particle sizes of the zeolites were estimated to be around 3  $\mu\text{m}$  and 6  $\mu\text{m}$  respectively. In addition, the successful formation of zeolites samples was verified using XRD, as shown in Fig. 1(c). The characteristic peaks and patterns of zeolite 5A were well-matched to those of the typical zeolite LTA framework reported in the literature[28]. In particular, the creation of hierarchical structures (containing both microporous

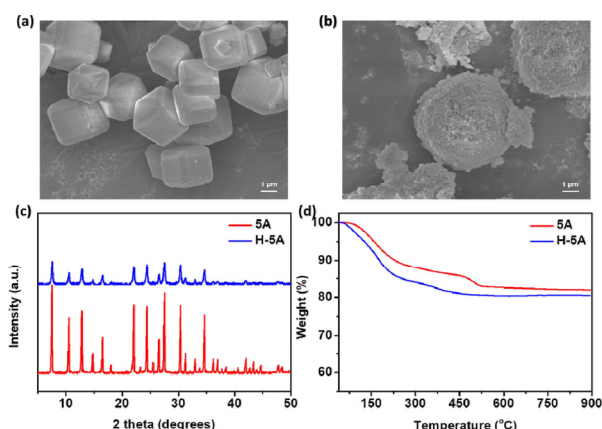


**Fig. 1.** Field emission-scanning electron microscope (FE-SEM) morphologies of (a) zeolite 5A and (b) hierarchical zeolite 5A; (c) X-ray diffraction (XRD) patterns of three zeolites; (d) Thermogravimetric analysis (TGA) curves of three zeolites in the 50~900°C range.

and mesoporous domains) generally resulted in a clear decrease in the peak intensity, as smaller fractions of zeolite domains can be expected. The feasibility of using zeolite 5A in membrane carbonization processes was assessed by evaluating its thermal stabilities from 50 to 900°C. A continuous weight loss which is attributed to the removal of water molecules that potentially resided in the samples was observed until 525°C was reached for all of the zeolite 5A materials. This result suggested that the integrity of zeolite frameworks can be maintained when these porous materials are heated to a carbonization temperature of Matrimid® 5218.

Further evaluation of zeolite 5A was conducted using N<sub>2</sub> physisorption isotherms at -196°C (77 K) in the P/P° range of 0~1, as demonstrated in Fig. 2(a). The analysis of the isotherms showed that all zeolites demonstrated high N<sub>2</sub> sorption at low partial pressure, which was a typical indication of a Type I isotherms (presence of large micropore volume). The presence of an hysteresis loop between the adsorption and desorption curves for the hierarchical zeolite 5A indicated the presence of mesopores, which were determined to be 8.3 nm according to the BJH algorithm[31] [Fig. 2(b)]. In comparison, the hierarchical zeolite 5A gave a comparatively lower N<sub>2</sub> sorption in comparison to zeolite 5A, which can be correlated with the surface

areas and micropore volumes computed using the Brunauer-Emmett-Teller (BET) theory and t-plot method, respectively (Table 1). This analysis was generally consistent with the decrease in peak intensity of hierarchical zeolite 5A seen in the XRD patterns.

The O<sub>2</sub> and N<sub>2</sub> adsorption properties of zeolite 5A were also evaluated using pure component gas adsorption isotherms, which determined the affinities for these two gases. As shown in Fig. 2(c), the O<sub>2</sub> adsorption was generally lower than that of N<sub>2</sub> in all of the synthesized zeolites. This is probably attributed to the higher polarizability of N<sub>2</sub> compared to O<sub>2</sub> ( $17.4 \times 10^{-25} \text{ cm}^3$  vs.  $15.8 \times 10^{-25} \text{ cm}^3$ ). Similar phenomena have been reported for other zeolite frameworks[32,33]. Based on the adsorbed amount, O<sub>2</sub> and N<sub>2</sub> adsorption can be generally correlated to the accessible surface areas evaluated by the N<sub>2</sub> physisorption measurement.

### 3.2. Properties of carbon molecular sieve membranes

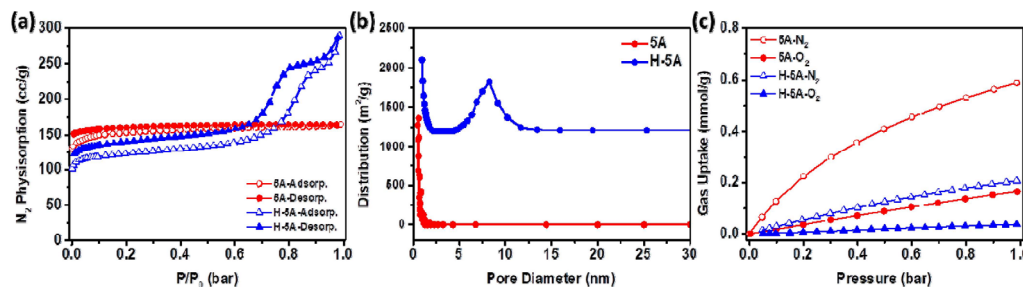
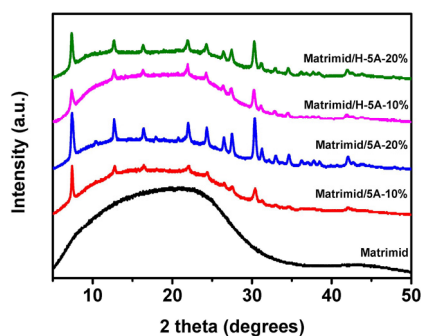
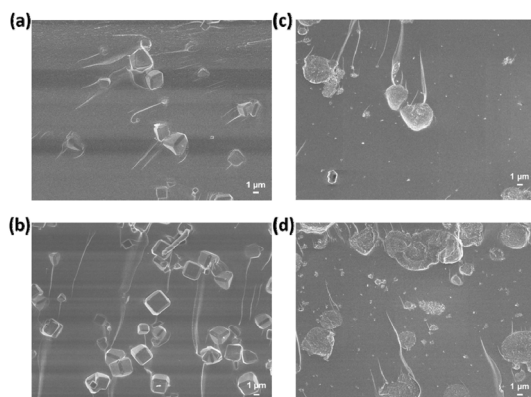
After the successful preparation of zeolite 5A, membrane precursors were developed by incorporating the zeolites into mixed-matrix membranes. As shown in Fig. 1(d), the zeolites were thermally stable up to 900°C, as no signs of structural degradation were observed. Moreover, the thermal stability of the zeolites after the carbonization of the membrane precursors was also apparent from the XRD results. As described in Fig. 3, the characteristic peaks of the zeolite 5A were identified, suggesting that the crystallinity of the zeolite 5A remained intact after the carbonization process.

Next, the cross-section morphologies of the carbon molecular sieve membranes were verified using FE-SEM (Fig. 4). In general, the *sieve-in-a-cage* morphology is a typical interfacial defect that occurs when inorganic fillers (especially zeolites) are incorporated into mixed-matrix membranes. Surprisingly, this phenomenon was not observed in this study. In fact, the interfacial voids between the zeolite 5A and Matrimid® 5218 membrane seemed to narrow, perhaps because of the conversion of the glassy material into a rubbery polymer matrix at the glass transition temperature (319

**Table 1.** Surface Areas and Micropore Volumes of All of Zeolites Calculated from the N<sub>2</sub> Physisorption Isotherm at 77 K

Fillers	$S_{BET}^a$ (m <sup>2</sup> /g)	$S_{Lang}^b$ (m <sup>2</sup> /g)	$S_{Micro}^c$ (m <sup>2</sup> /g)	$V_{Micro}^d$ (cc/g)
Zeolite 5A	779.0	810.4	750.7	0.3168
H-Zeolite 5A	476.7	561.9	398.7	0.1706

Notes: <sup>a</sup> Surface areas were computed using the BET theory at  $P/P^0 = 0.05\text{--}0.2$ , <sup>b</sup> Surface areas were calculated using the Langmuir equation at  $P/P^0 = 0.05\text{--}0.2$ , <sup>c,d</sup> Micropore areas and volumes were computed using the t-plot method at  $P/P^0 = 0.4\text{--}0.6$ .

**Fig. 2.** (a) N<sub>2</sub> physisorption isotherms of zeolites measured at -196°C (77 K) under the  $P/P^0$  range of 0 to 1. (b) Pore size distribution of zeolites, which were determined via a BJH method. (c) O<sub>2</sub> and N<sub>2</sub> adsorption isotherms of zeolites at 35°C.**Fig. 3.** XRD patterns of carbon molecular sieve membranes derived from pure Matrimid<sup>®</sup> 5218 and mixed-matrix membranes.**Fig. 4.** FE-SEM images of cross-sections of CMSMs; zeolite 5A (a) 10 wt%, (b) 20 wt%; H-zeolite 5A (c) 10 wt%, (d) 20 wt%.

°C), prior to the carbonization process[34]. During this process, the polymer chains had sufficient flexibility to undergo thermal rearrangement to heal the interfacial voids that occurred at a higher temperature (550°C). Nonetheless, it is still difficult to completely seal the interfacial voids, such that microscopically invisible nanogaps at the carbon/zeolite 5A interfaces may still be present.

### 3.3. O<sub>2</sub>/N<sub>2</sub> separation performance of carbon molecular sieve membranes

The O<sub>2</sub>/N<sub>2</sub> separation performance of the carbon molecular sieve membranes was evaluated at 35°C and 1 bar by the mixture gas permeation testing (Table 2). As compared to pure Matrimid<sup>®</sup> 5218 precursor membrane (before carbonization)[35], pure Matrimid<sup>®</sup> 5218 CMSM showed an enhanced O<sub>2</sub> permeability (4.8 barrer) with marginal dip in O<sub>2</sub>/N<sub>2</sub> selectivity (5.64). In addition, the O<sub>2</sub>/N<sub>2</sub> separation results for the pure Matrimid<sup>®</sup> 5218 CMSM were comparable with the data in the literature which reports the O<sub>2</sub> permeability of 5 barrer and the O<sub>2</sub>/N<sub>2</sub> selectivity of 6[36]. Meanwhile, it was observed that the incorporation of either zeolites 5A or H-zeolite 5A into the carbon molecular sieve membranes dramatically improved the O<sub>2</sub> permeability.

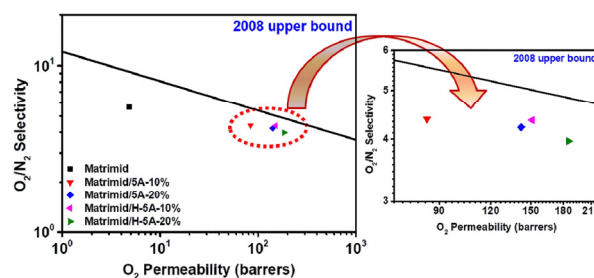
**Table 2.** Mixture Gas Permeation Data Measured at 35°C and 1 bar Upstream Pressure ( $O_2/N_2 = 21/79$ ) for CMSMs derived from Pure Matrimid<sup>®</sup> 5218 and Mixed-Matrix Precursors

Membrane	$O_2$ permeability <sup>a</sup> (barrer)	$O_2/N_2$ selectivity
Matrimid <sup>®</sup> 5218	$4.8 \pm 0.2$	$5.64 \pm 0.13$
Matrimid <sup>®</sup> 5218/Zeolite 5A-10%	$84 \pm 4$	$4.38 \pm 0.16$
Matrimid <sup>®</sup> 5218/Zeolite 5A-20%	$142 \pm 3$	$4.22 \pm 0.08$
Matrimid <sup>®</sup> 5218/H-zeolite 5A-10%	$151 \pm 9$	$4.36 \pm 0.16$
Matrimid <sup>®</sup> 5218/H-zeolite 5A-20%	$185 \pm 6$	$3.96 \pm 0.04$

<sup>a</sup> 1 barrer =  $10^{-10} \text{ cm}^3_{STP} \cdot \text{cm} / \text{cm}^2 \cdot \text{s} \cdot \text{cmHg}$

On the other hand, incorporation of H-zeolite 5A achieved an exceptional enhancement in  $O_2$  permeability, reaching a high  $O_2$  permeability of 185 barrers with only a slight decrease in  $O_2/N_2$  selectivity. It should be noted that the overall accessible surface area for H-zeolite 5A was the lowest among the three zeolites (Table 1). Accordingly, the mesopores were the most probable transport pathways for rapid  $O_2$  diffusion, supplementary to the presence of intrinsic micropores in the zeolite 5A. This is demonstrated by the exceptional enhancement in  $O_2$  permeability (37.5-fold) for Matrimid<sup>®</sup> 5218/H-zeolite 5A-20% compared with its nascent membrane. It gives a better performance than zeolite 5A under the same particle loading (20%), with 28.6-fold of enhancement has been reported. Although  $O_2/N_2$  selectivity was slightly decreased with the Matrimid<sup>®</sup> 5218/H-zeolite 5A, the overall  $O_2/N_2$  selectivity was still comparable across zeolites with different particle sizes.

To investigate the success of our optimal design of the filler properties (particle size and pore size) in carbon molecular sieve membranes, the gas permeation results were compared and plotted against the upper bound limit for  $O_2/N_2$  separation. The comparison clearly showed that it was generally challenging for current CMSM to surpass the 2008 upper bound limit[12], as demonstrated in Fig. 5, probably because of the low performance of the porous carbon matrix derived from Matrimid<sup>®</sup> 5218. In addition, considering the fact that zeolites preferentially absorb  $N_2$  over  $O_2$ , there is a possibility of decreased in  $O_2/N_2$  selectivity in mixed-matrix CMSM. In this regard, it is important to empha-

**Fig. 5.** Robeson plot comparing the  $O_2$  permeabilities and  $O_2/N_2$  selectivities of carbon molecular sieve membranes.

size that although our strategy was unable to completely reverse the trade-off phenomenon, the extraordinary enhancement in  $O_2$  permeability by the incorporation of H-zeolite 5A into CMSM alleviated the shortcoming of the trade-off relationship, as demonstrated by a gentler decrease in selectivity. Clearly, this approach drastically improved the overall  $O_2/N_2$  separation performance relative to the pure CMSM. This implies that a performance beyond the upper bound can potentially be realized by using a different polymer precursor that gives higher  $O_2/N_2$  selectivity instead of the inexpensive commercial polymer used in this study. However, using such precursor would inevitably increase the cost of membrane production.

#### 4. Conclusion

Mixed-matrix CMSM containing zeolite 5A with various structural properties were synthesized for enhanced  $O_2/N_2$  separation. In general, incorporating 5A fillers into CMSM dramatically increased the permeability of the membrane with marginal sacrifices in selectivity.

Thus, the study of the investigation of hierarchical porous structure were conducted in a systematic manner. Interestingly, hierarchical zeolite 5A, which contains both microporous and mesoporous domains, improved the performance even further, indicating that the mesopores in the zeolite can serve as an additional pathway for rapid gas diffusion. This strategy is facile yet effective in improving the gas permeability in a cost-effective way and producing high performance membranes based on readily available, inexpensive membrane materials such as commercial polymer and zeolites.

### Acknowledgements

This research is supported by the National Research Foundation, Prime Minister's Office, Singapore, and the National Environment Agency, Ministry of the Environment and Water Resources, Singapore, under the Waste-to-Energy Competitive Research Programme (WTE CRP 1601 105). T.-H. Bae would also like to thank Korea Advanced Institute of Science and Technology for the financial support.

### Reference

1. P. Baskar and A. Senthilkumar, "Effects of oxygen enriched combustion on pollution and performance characteristics of a diesel engine", *Eng. Sci. Technol. Int. J.*, **19**, 438 (2016).
2. D. Gielen, "CO<sub>2</sub> removal in the iron and steel industry", *Energy Convers. Manag.*, **44**, 1027 (2003).
3. R. Chen and W. Yeun, "Review of the high-temperature oxidation of iron and carbon steels in air or oxygen", *Oxid. Met.*, **59**, 433 (2003).
4. M. S. Rahman and C. O. Perera, "Drying and food preservation", In *Handbook of Food Preservation*, p. 173, Marcel Dekker, New York (1999).
5. R. Cornelissen and G. Hirs, "Exergy analysis of cryogenic air separation", *Energy Convers. Manag.*, **39**, 1821 (1998).
6. Y. Zhu, X. Liu, and Z. Zhou, "Optimization of cryogenic air separation distillation columns", In *Proceedings of 2006 6th World Congress on Intelligent Control and Automation*, p. 7702 (2006).
7. A. Smith and J. Klosek, "A review of air separation technologies and their integration with energy conversion processes", *Fuel Process. Technol.*, **70**, 115 (2001).
8. D. Ruthven and S. Farooq, "Air separation by pressure swing adsorption", *Gas Sep. Purif.*, **4**, 141 (1990).
9. M. Hassan, D. Ruthven, and N. Raghavan, "Air separation by pressure swing adsorption on a carbon molecular sieve", *Chem. Eng. Sci.*, **41**, 1333 (1986).
10. L. Jiang, L. T. Biegler, and V. G. Fox, "Simulation and optimization of pressure-swing adsorption systems for air separation" *AIChE J.*, **49**, 1140 (2003).
11. L. M. Robeson, "The upper bound revisited", *J. Membr. Sci.*, **320**, 390 (2008).
12. L. M. Robeson, "Correlation of separation factor versus permeability for polymeric membranes", *J. Membr. Sci.*, **62**, 165 (1991).
13. H. B. Park, C. H. Jung, Y. M. Lee, A. J. Hill, S. J. Pas, S. T. Mudie, E. Van Wagner, B. D. Freeman, and D. J. Cookson, "Polymers with cavities tuned for fast selective transport of small molecules and ions", *Science*, **318**, 254 (2007).
14. R. Swaidan, X. Ma, E. Litwiller, I. Pinnau, "High pressure pure-and mixed-gas separation of CO<sub>2</sub>/CH<sub>4</sub> by thermally-rearranged and carbon molecular sieve membranes derived from a polyimide of intrinsic microporosity", *J. Membr. Sci.*, **447**, 387 (2013).
15. R. Kumar and W. J. Koros, "High performance carbon molecular sieve membranes resistance to aggressive feed stream contaminants", *Ind. Eng. Chem. Res.*, **58**, 6740 (2019).
16. W. Salleh, A. Ismail, T. Matsuura, and M. Abdullah, "Precursor selection and process conditions in the preparation of carbon membrane for gas separation: A review", *Sep. Purif. Rev.*, **40**, 261 (2011).
17. W. Salleh and A. Ismail, "Effects of carbonization heating rate on CO<sub>2</sub> separation of derived carbon



- membranes”, *Sep. Purif. Technol.*, **88**, 174 (2012).
18. C. Zhang, Y. Dai, J. R. Johnson, O. Karvan, and W. J. Koros, “High performance ZIF-8/6FDA-DAM mixed matrix membrane for propylene/propane separations”, *J. Membr. Sci.*, **389**, 34 (2012).
  19. H. Gong, C. Y. Chuah, Y. Yang, and T.-H. Bae, “High performance composite membranes comprising Zn(pyrz)<sub>2</sub>(SiF<sub>6</sub>) nanocrystals for CO<sub>2</sub>/CH<sub>4</sub> separation”, *J. Ind. Eng. Chem.*, **60**, 279 (2018).
  20. B. Zhang, Y. Shi, Y. Wu, T. Wang, and J. Qiu, “Towards the preparation of ordered mesoporous carbon/carbon composite membranes for gas separation” *Sep. Sci. Technol.*, **49**, 171 (2014).
  21. L. Li, T. Wang, Q. Liu, Y. Cao, and J. Qiu, “A high CO<sub>2</sub> permselective mesoporous silica/carbon composite membrane for CO<sub>2</sub> separation”, *Carbon*, **50**, 5186 (2012).
  22. X. Yin, N. Chu, J. Yang, J. Wang, and Z. Li, Thin zeolite T/carbon composite membranes supported on the porous alumina tubes for CO<sub>2</sub> separation”, *Int. J. Greenh. Gas Con.*, **15**, 55 (2013).
  23. P. S. Tin, T.-S. Chung, L. Jiang, and S. Kulprathipanja, “Carbon-zeolite composite membranes for gas separation”, *Carbon*, **43**, 2025 (2005).
  24. X. Yin, J. Wang, N. Chu, J. Yang, J. Lu, Y. Zhang, and D. Yin, “Zeolite L/carbon nanocomposite membranes on the porous alumina tubes and their gas separation properties”, *J. Membr. Sci.*, **348**, 181 (2010).
  25. C. Y. Chuah, K. Goh, Y. Yang, H. Gong, W. Li, H. E. Karahan, M. D. Guiver, R. Wang, and T.-H. Bae, “Harnessing filler materials for enhancing biogas separation membranes”, *Chem. Rev.*, **118**, 8655 (2018).
  26. A. Corma, “From microporous to mesoporous molecular sieve materials and their use in catalysis”, *Chem. Rev.*, **97**, 2373 (1997).
  27. C. Y. Chuah, K. Goh, and T.-H. Bae, “Hierarchically structured HKUST-1 nanocrystals for enhanced SF<sub>6</sub> capture and recovery”, *J. Phys. Chem. C*, **121**, 6748 (2017).
  28. T. H. Nguyen, S. Kim, M. Yoon, and T. H. Bae, “Hierarchical zeolites with amine-functionalized mesoporous domains for carbon dioxide capture”, *ChemSusChem*, **9**, 455 (2016).
  29. W. Li, S. Samarasinghe, and T.-H. Bae, “Enhancing CO<sub>2</sub>/CH<sub>4</sub> separation performance and mechanical strength of mixed-matrix membrane via combined use of graphene oxide and ZIF-8”, *J. Ind. Eng. Chem.*, **67**, 156 (2018).
  30. T. H. Bae, J. S. Lee, W. Qiu, W. J. Koros, C. W. Jones, and S. A. Nair, “High-performance gas-separation membrane containing submicrometer-sized metal-organic framework crystals”, *Angew. Chem. Int. Ed.*, **49**, 9863 (2010).
  31. C. Y. Chuah, S. Yu, K. Na, and T.-H. Bae, “Enhanced SF<sub>6</sub> recovery by hierarchically structured MFI zeolite”, *J. Ind. Eng. Chem.*, **62**, 64 (2018).
  32. J.-R. Li, R. J. Kuppler, and H.-C. Zhou, “Selective gas adsorption and separation in metal-organic frameworks”, *Chem. Soc. Rev.*, **38**, 1477 (2009).
  33. S. Nandi and P. Walker Jr, “Separation of oxygen and nitrogen using 5A zeolite and carbon molecular sieves”, *Sep. Sci. Technol.*, **11**, 441 (1976).
  34. F. Weigelt, P. Georgopoulos, S. Shishatskiy, V. Filiz, T. Brinkmann, and V. Abetz, “Development and characterization of defect-free matrimid<sup>®</sup> mixed-matrix membranes containing activated carbon particles for gas separation”, *Polymers*, **10**, 51 (2018).
  35. C. Y. Chuah and T.-H. Bae, “Incorporation of Cu<sub>3</sub>BTC<sub>2</sub> nanocrystals to increase the permeability of polymeric membranes in O<sub>2</sub>/N<sub>2</sub> separation”, *BMC Chem. Eng.*, **1**, 2 (2019).
  36. A. Fuertes, D. Nevskaja, and T. Centeno, “Carbon composite membranes from Matrimid<sup>®</sup> and Kapton<sup>®</sup> polyimides for gas separation”, *Micropor. Mesopor. Mater.*, **33**, 115 (1999).